Single-Phase to Six-Phase (AC-DC-AC) Converter for Traction

Anup Kumar(✉), Mohan V. Aware, B. S. Umre, and Manoj A. Waghmare

Department of Electrical Engineering, Visvesvaraya National Institute of Technology, Nagpur, India
anup4321kumar@gmail.com, {mvaware,bsumre}@eee.vnit.ac.in

Abstract. Power quality issues and drive performance under dynamic conditions are the major concern in traction. This paper proposes an active front-end converter (AFEC) fed 6-ϕ voltage source inverter (VSI) driven induction motor (IM) drive for traction. The AFEC at the 1-ϕ grid side and 6-ϕ VSI at the induction motor side are controlled independently. The proposed converter overcomes the power quality issues associated with the 1-ϕ diode bridge rectifier fed VSI-driven induction motor drive and enhances the drive performance by reducing the torque ripple. The control technique adopted over a 1-ϕ AFEC maintains UPF operation at the grid side and DC-bus voltage is maintained constant under different loading conditions of the induction motor drive. Moreover, the proposed technique adopted over the AFEC mitigates 2f oscillation of the DC-bus voltage. The simulation and experimental results are presented to evaluate the proposed converter's performance and control technique.

Keywords: Active front-end converter · UPF · DC-bus voltage control · 2f oscillation · THD

1 Introduction

A 1-ϕ grid-connected AC-DC converter has drawn the attention of researchers and industrial people towards their potential application in electric multiple units (EMUs) [1, 2]. The traction system consists of a traction substation, catenary, pantograph, and electric multiple units (EMUs). The 2f oscillation over voltage that causes blockage in the EMUs is the main problem associated with the traction network [3, 4]. The main cause of 2f oscillation is the mismatching of parameters between the electrical quantities of the traction network and the control variables of the traction power converters. To suppress 2f oscillation, different control techniques are adopted in the literature [5].

The auto disturbance rejection control (ADRC) is proposed to suppress 2f oscillation in [6]. The ADRC has the inherent advantage of excellent adaptability and robustness. The ADRC has good control performance when the inner parameters of the controlled object are changed.

A typical EMU traction system that employs PWM rectifiers achieves sinusoidal source current, UPF, and stable DC-bus voltage. In EMU PWM rectifiers, DC current

S. Sugiman et al. (Eds.): MIMSE-M-E 2022, AER 216, pp. 132–140, 2023.
https://doi.org/10.2991/978-94-6463-078-7_15

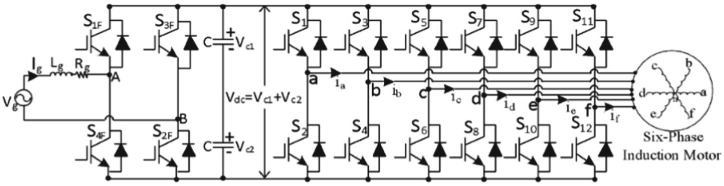

Fig. 1. Schematic diagram of 1-ϕ to 6-ϕ (AC-DC-AC) converter fed IM drive.

injects because of the inconsistent switching characteristics and 2nd harmonic voltage on the transformer's primary side. The DC current saturates the core of the transformer and distorts the source current. The current controller in EMU PWM rectifiers can solve the problems highlighted below.

1. Source current shaping
2. Mitigation of the lower-order harmonics from the grid current.
3. Eliminate the DC current avoiding the transformer core saturation.

Different topologies of 1-ϕ to 3-ϕ (AC-DC-AC) converters are studied in the literature [7–9]. State-of-the-art 1-ϕ to 3-ϕ (AC-DC-AC) converters are discussed in [10]. A 1-ϕ AFEC fed 3-ϕ VSI-driven induction motor drive overcomes all the drawbacks associated with the diode bridge-fed VSI. However, the advantages associated with multi-phase drives add more robustness and reliability to their counterparts [11, 12]. The various advantages of the multi-phase induction motor mentioned in the literature led to the motivation toward the 1-ϕ to a 6-ϕ power converter for traction.

The schematic diagram of a 1-ϕ to a 6-ϕ (AC-DC-AC) converter is shown in Fig. 1. In a 1-ϕ to 6-ϕ converter two converters are cascaded in which the output of a single-phase active front-end converter (AFEC) is the input to the 6-ϕ VSI fed IM drive. The multiphase VSI fed induction motor has some distinct advantages: torque ripple reduction, per-phase voltage rating of the switch reduced, and fault-tolerant operation. The applications of such drives are traction and ship propulsion.

This paper proposes an independent control technique to control 1-ϕ AFEC on the grid side and 6-ϕ induction motor on the VSI side. A closed-loop control technique is proposed to control the AFEC at the grid side and an open-loop V/f control technique is adopted on a 6-ϕ VSI-fed IM drive. The main advantage of the independent control technique is that the modulating signals for switching the power converters at the grid and load side are decoupled. Therefore, disturbance at the IM side doesn't affect the power converter performance on the grid side.

This manuscript is arranged as follows. In Sect. 2, control of 1-ϕ to 6-ϕ VSI is discussed. In Sect. 3, the simulation results of the proposed research work are presented.

The experimental results are presented in Sect. 4. The conclusion of the proposed work is discussed in Sect. 5.

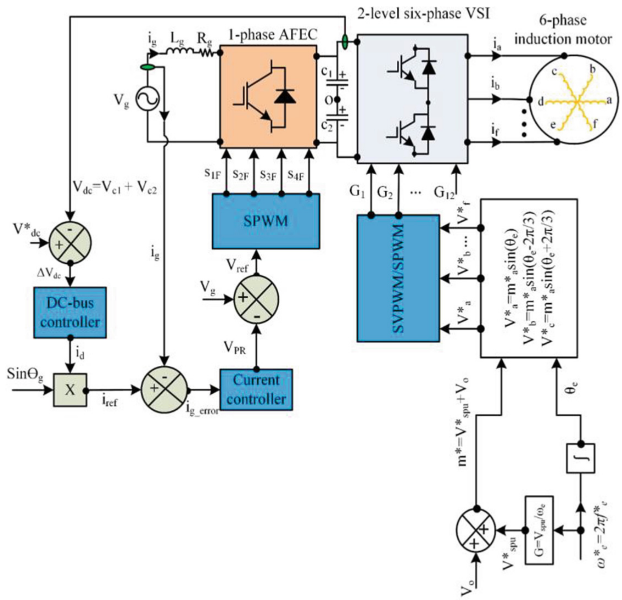

Fig. 2. Control technique of 1-ϕ to 6-ϕ (AC-DC-AC) converter fed induction motor drive.

2 Control Technique of 1-ϕ to 6-ϕ Converter

The control technique of 1-ϕ to 6-ϕ (AC-DC-AC) converter involves a closed-loop control technique at the front-end side and an open-loop V/f control technique at the 6-ϕ IM drive. The control technique of the complete system is shown in Fig. 2.

2.1 Control Technique of 1-ϕ AFEC

The control of a 1-ϕ AFEC consists of two loops. The DC bus voltage control loop is an outer loop and the current control loop is an inner loop. The outer loop controls the DC bus voltage to the set reference voltage (V*dc). Moreover, a single-phase phase-locked loop (PLL) is required to estimate the grid voltage phase-angle and frequency. The phase angle estimated by the PLL is used to synthesize the reference current (I*ref). The block diagram of analysis shows that the system is stable.

The average model of the control technique is shown in Fig. 3(a). In the average model, the current controller gain is considered as unity. The controller gains are defined in (1)–(2) [13].

$$k_v = \frac{\sqrt{2}CV_{dc}}{V_{rms}T_v} \tag{1}$$

$$k = \frac{V_{rms}T_v}{\sqrt{2}V_{dc}} \tag{2}$$

Where Tv = 0.25 s is the time constant of the DC-bus voltage loop, C is the capacitance of the DC-bus capacitor in µF, and Vrms is the RMS value of the grid voltage in V.

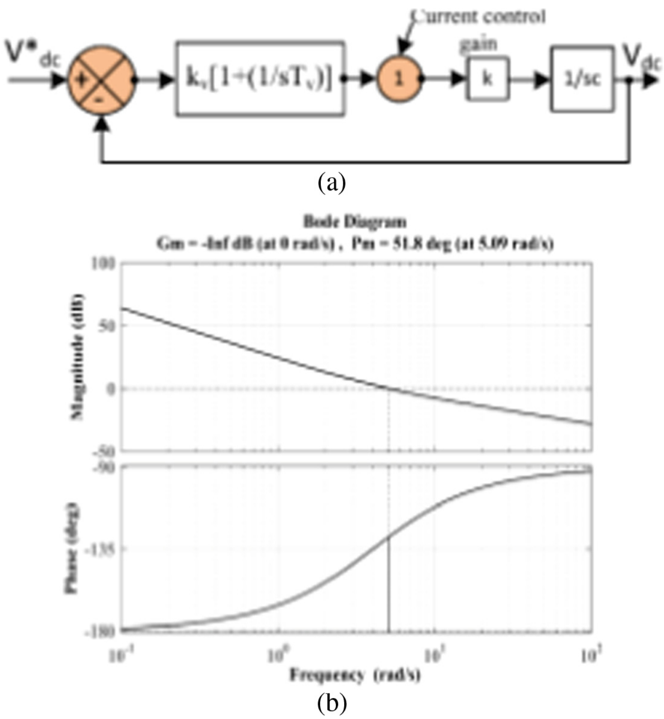

Fig. 3. (a) Average model of the control technique. (b) Bode plot of the DC bus voltage control loop.

The open loop transfer function of the DC-bus voltage control loop is given in (3).

$$G_{(s)} = \frac{k_v K T_v s + k_v k}{s^2 T_v C} \tag{3}$$

Substituting the value of the controller gains in (3) yield (4).

$$G_{(s)} = \frac{0.0094_s + 0.0376}{0.0235^2} \tag{4}$$

The Bode plot analysis of the DC-bus voltage control loop represented by (4) is shown in Fig. 3(b). The Bode plot analysis shows that the system is stable.

2.2 Open-Loop V/f Control Technique of 6-ϕ VSI Driven Induction Motor

The control of stator frequency (fe) is essential for the variable frequency drive (VFD). In volt/Hz (V/fe) control, the IM stator terminal voltage is required to be proportional to stator frequency (fe) so that the flux (ψ) remains constant, neglecting the stator resistance (Rs) drop. The V/fe control technique of 1-φ to 6-φ (AC-DC-AC) converter-fed induction motor drive is shown in Fig. 2. The modulating signals (V*a,V*b,…, and V*f) are directly generated from the frequency command (f*e) by the gain factor (G) to maintain the ψ constant [14]. The gain factor is given in (5).

$$G = \frac{1}{\omega e} \times V_{spu} \tag{5}$$

At low speed, the stator frequency (fe) becomes small, the stator resistance tends to absorb the major amount of stator voltage, thus weakening the flux. The boost voltage (Vo) is added so that the rated flux and corresponding full load torque become available down to zero speed. The effect of Vo becomes negligible at higher frequencies.

3 Simulation Results

The simulation parameters are given in Table 1. The switching frequency is 10 kHz at 1-φ AFEC and 6-φ VSI sides. The motor parameters are given in Table 2. The reference DC-bus voltage (V*dc) is set at 200 V. The source voltage and current and the DC-bus voltage under different loading conditions of the induction motor are shown in Fig. 4(a). It is evident from this figure that the UPF operation is achieved on the grid side.

Table 1. Simulation parameters.

Symbol	Description	Value	unit
V^*dc	reference dc link voltage	200	V
C	DC-bus capacitor	4700	μF
Vg	grid voltage	100	v
fg	grid frequency	50	HZ
Lg	grid inductance	7	mH
Rg	grid resistance	1	Ω
fs	switching frequency	10	kHz

Table 2. 6-Φ Induction Motor Parameter

Symbol	Description	Value	Unit
R_S, Rr	stator and rotor resistance	5.17, 2.3	Ω
L_{ls}, Llr	stator & rotor leakage inductance	20.8	mH
Lm	magnetic inductance	215	mH
Pr	Motor rated power	1.5	kW
ϕr	rated flux	0.35	wb
P	pole pairs	2	-
R_S, Rr	magnetic inductance	5.17, 2.3	Ω

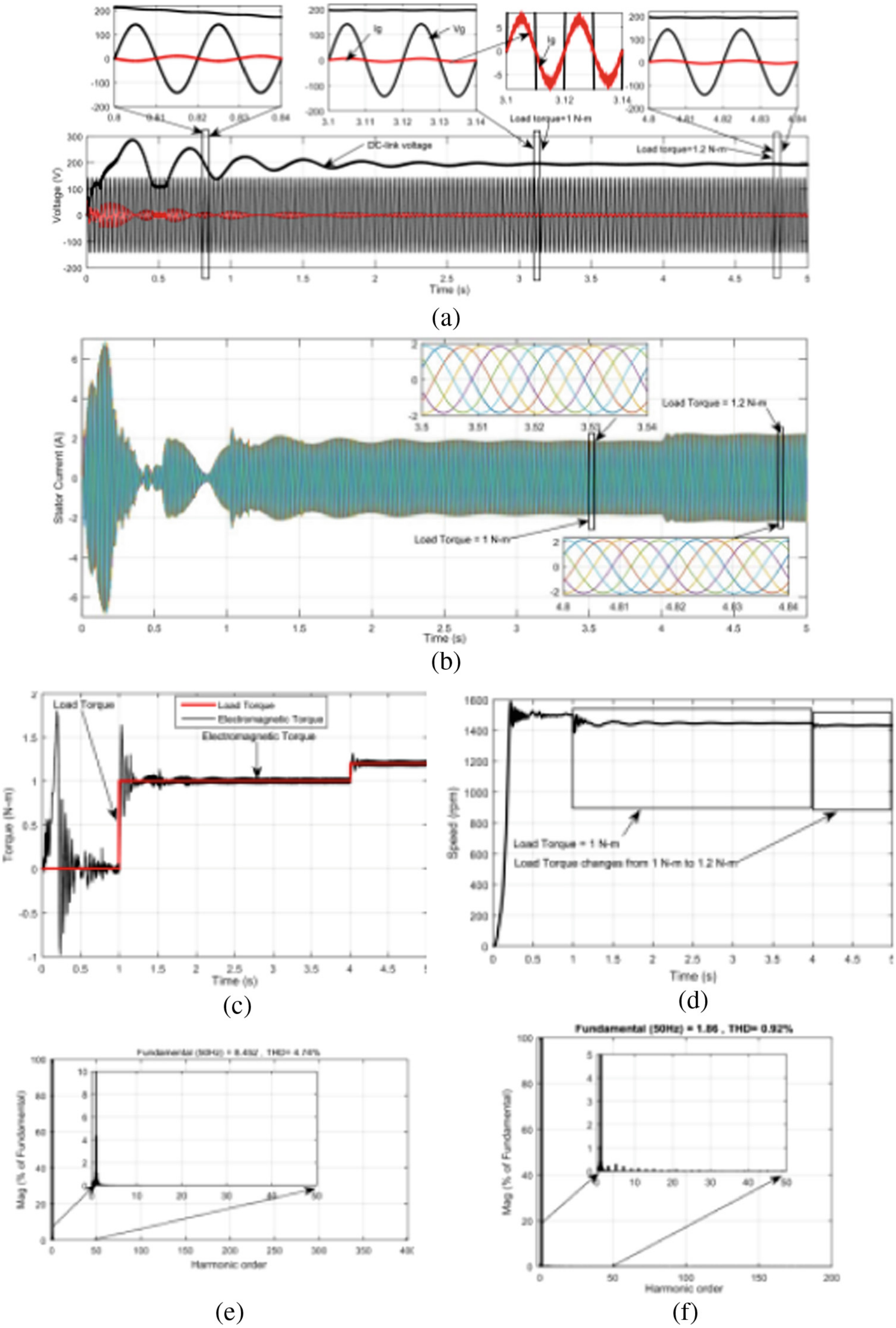

Fig. 4. Simulation results of 1-ϕ to 6-ϕ converter for IM. (a) Grid voltage and current and DC-bus voltage. (b) Stator current. (c) Electromagnetic torque. (d) Speed. (e) FFT analysis of the grid current. (f) FFT analysis of the phase current.

The stator current over the entire range of operation of the IM drive is shown in Fig. 4(b). The electromagnetic torque and speed of the induction motor under different loading conditions are shown in Fig. 4(c) and (d) respectively. The FFT analysis of the grid current and stator current is shown in Fig. 4(e) and (f) respectively. The grid current THD is 4.74% and the phase current THD is 0.92%.

4 Experimental Results

A laboratory prototype model of a 1-ϕ to a 6-ϕ VSI-driven IM drive is designed and developed in the laboratory. The prototype model is tested for a power rating equal to 250 W. The control algorithm of the complete system is developed on TMS320F28379D DSP Launchpad. The switching and sampling frequencies are 10 kHz and 20 kHz respectively.

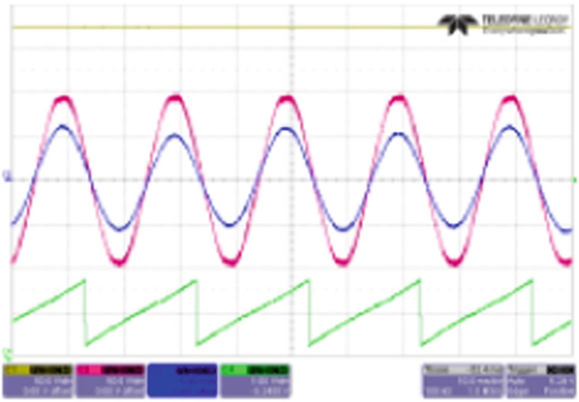

(a)

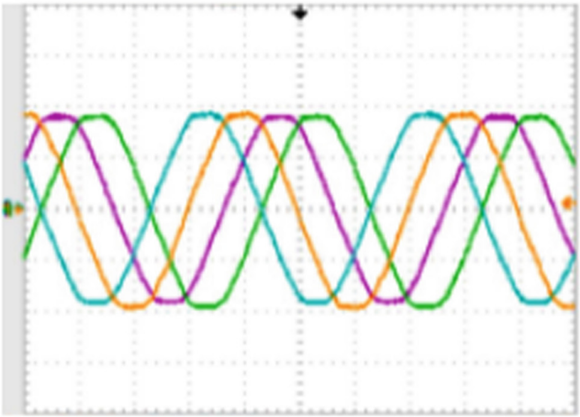

(b)

Fig. 5. Experimental results. (a) Grid voltage, current, DC-bus voltage, and grid voltage phase-angle. C1 (yellow): DC-bus voltage (50 V/div), C2 (red): grid voltage (50 V/div), C3 (blue): grid current (5A/div), C4 (green): grid voltage phase-angle. X-axis-(Time): 20ms/div. (b) Stator currents (ia, ib, ic, and id) of the VSI-fed 6-φ IM drive.

The grid voltage and current are shown in Fig. 5(a). The UPF operation is shown in this figure. The DC-bus voltage is shown in Fig. 5(a). The experimental result shows that the proposed control technique is capable to eliminate 2f oscillation in the DC-bus voltage. A single-phase SOGI-PLL is used to estimate the grid voltage phase-angle, which is shown in Fig. 5(a). The stator currents (ia, ib, ic, and id) of the six-phase VSI-fed IM drive are shown in Fig. 5(b).

5 Conclusion

The control technique adopted over a 1-ϕ to a 6-ϕ VSI fed IM drive is capable to achieve the UPF operation at the grid side while maintaining the DC-bus voltage constant under different loading conditions of the IM drive. The 2f oscillation in the DC-bus voltage is mitigated by the appropriate selection of the bandwidth of the DC-bus voltage control loop. The efficacy of the proposed control technique is evaluated through the simulation and experimental results.

Acknowledgment. This research work is financially supported by the DST SERB.

References

1. Liu, Z., Zhang, G., Liao, Y.: Stability research of high-speed railway EMUs and traction network cascade system considering impedance matching, IEEE Trans. on Indus. Appl., vol. 52, no. 5, pp. 4315–4326, Sept.–Oct. (2016).
2. Brenna, M., Foiadelli, F., Zaninelli, D.: New stability analysis for tuning PI controller of power converters in railway application, IEEE Trans. on Indus. Electron., vol. 58, no. 2, pp. 533–543, Feb (2011).
3. Wang, H., Mingli, W., Sun, J.: Analysis of low-frequency oscillation in electric railways based on small-signal modeling of vehicle grid system in dq Frame, IEEE Trans. on Power Electron., vol. 30, no. 9, pp. 5318–5330, Sept (2015).
4. Zhang, G., Liu, Z., Yao, S., Liao, Y., Xiang, C.: Suppression of low frequency oscillation in traction network of high-speed railway based on auto-disturbance rejection control. IEEE Trans. on Transport. Elect., vol. 2, no. 2, pp. 244–255, June (2016).
5. Liu, Z., Yan, Q., Tasiu, I. A., Zhang, Y., Hu, K., Dragičević, T.: A model predictive control considering parameters and system uncertainties for suppressing low-frequency oscillations of traction dual rectifiers," IEEE Transactions on Transportation Electrification, vol. 7, no. 3, pp. 1031–1046, Sept. (2021).
6. Cecati, C., Dell'Aquila, A., Liserre, M., Monopoli, V. G.: Design of H-bridge multilevel active rectifier for traction systems, IEEE Trans. on Indus. Appl., vol. 39, no. 5, pp. 1541–1550, Sept.-Oct (2003).
7. Dewan, S., Showleh, M.: A novel static single-to-three-phase converter, IEEE Trans. magn., vol. 17, no. 6, pp. 3287–3289, Nov (1981).
8. dos Santos, E. C., Rocha, N., Jacobina, C. B.: Suitable single-phase to three-phase AC–DC–AC power conversion system, IEEE Trans. on Power Electron., vol. 30, no. 2, pp. 860–870, Feb. 2015.

9. Kumar, A., Aware, M. V., Umre, B. S.: Single-phase to three-phase power converter with reduced DC-link voltage ripple and grid current harmonics, IEEE Trans on Industry Appl., vol. 57, no. 1, pp. 664–672, Jan.–Feb (2021).
10. Santos, E. C., Jacobina, C. B., Silva, E. R.: Single-phase to three phase power converters: state of the art, IEEE Trans. Power Electron., vol. 27 (2012).
11. Levi, E.: Multiphase electric machines for variable-speed applications, IEEE Trans. on Ind. Electron., vol. 55, no. 5, pp. 1893–1909, May (2008).
12. González-Prieto, A., González-Prieto, I., Yepes, A. G., Duran, M. J., Doval-Gandoy, J.: On the advantages of symmetrical over asymmetrical multiphase AC drives with even phase number using direct controllers, IEEE Trans. on Ind. Electron., vol. 69, no. 8, pp. 7639–7650, Aug (2022).
13. Kumar, A., Aware, M. V., Umre, B. S., Waghmare, M. A.: Comparative performance analysis of single-phase grid-connected converters, 2021 IEEE 2nd International conference on smart technologies for power, energy, and control (STPEC), pp. 1–6 (2021).
14. Bimal, K. B.: Modern power electronics and AC drives.: PHI Learning (2011).